

## Theory of electromagnetic modes of magnetic effective-medium films

This article has been downloaded from IOPscience. Please scroll down to see the full text article.

1997 J. Phys.: Condens. Matter 9 1039

(<http://iopscience.iop.org/0953-8984/9/5/010>)

View [the table of contents for this issue](#), or go to the [journal homepage](#) for more

Download details:

IP Address: 171.66.16.207

The article was downloaded on 14/05/2010 at 06:15

Please note that [terms and conditions apply](#).

# Theory of electromagnetic modes of magnetic effective-medium films

F G Elmezghi† and R E Camley‡

Department of Physics, University of Essex, Colchester, Essex CO4 3SQ, UK

Received 29 May 1996, in final form 23 September 1996

**Abstract.** We study the surface and guided wave polaritons for a magnetic layered structure on a substrate. Using the effective-medium approximation we obtain analytic equations for implicit dispersion relations. These dispersion relations are solved numerically for a variety of layering patterns, and profiles showing the localization of both guided waves and surface waves are obtained. Explicit results are presented for an  $\text{FeF}_2$ – $\text{ZnF}_2$  superlattice on a  $\text{ZnF}_2$  substrate.

## 1. Introduction

Polaritons, electromagnetic waves coupled to the elementary excitations of a crystal such as phonons, plasmons and magnons, are a topic of continuing interest [1, 2]. In thin films one finds both surface polaritons, in which the excitation is localized near the surface, and guided modes, where the excitation has a standing-wave-like character within the film. Polaritons in semiconducting media have been extensively examined. For example, Ushioda and Loudon treated the surface and guided modes for electromagnetic waves coupled to the optical phonon in semiconductor films [3]. Surface polariton and related modes that propagate in thin-film magnetoplasmas have been studied extensively by Kushwaha and Halevi [4–7]. Recently, a full discussion of surface and guided waves in the retarded limit for magnetoplasma films was given by Elmezghi and Tilley [8]. A substantial account of an effective-medium treatment of layered magnetoplasma films has recently been given by Elmezghi [9].

Excitations in magnetic films have been investigated by a number of authors, e.g. for the case of a ferromagnetic slab by Damon and Eshbach [10], Karsono and Tilley [11] and Marchand and Caille [12]. Early theoretical work on surface polaritons on antiferromagnetics [13–15] has now been verified experimentally for  $\text{FeF}_2$  both through infra-red reflectivity [16–18] and through infra-red attenuated total reflection (ATR) measurements [19]. This experimental work gives a renewed impetus to extend theoretical calculations to more complex and realistic structures.

In recent years, there has been a surge of interest in multilayer structures. Multilayers composed of two antiferromagnets such as  $\text{FeF}_2$ – $\text{CoF}_2$  [20] and  $\text{NiO}$ – $\text{CoO}$  [21] have been constructed and studied by neutron scattering and by thermal measurements. In addition, individual ultra-thin antiferromagnetic films can be studied by producing many of them in an antiferromagnetic–nonmagnet structure such as  $\text{CoO}$ – $\text{MgO}$  [22]. It is likely that these

† Permanent address: Department of Physics, Al-Fatah University, Post Box 13450 Tripoli, Libya.

‡ Permanent address: Department of Physics, University of Colorado at Colorado Springs, Colorado Springs, CO 80933-7150, USA.

structures will eventually be characterized by infra-red measurements and therefore it is necessary to have a theoretical understanding of the polariton modes in these structures.

The magnetostatic spin wave modes in superlattices were originally obtained [23] by using Bloch's theorem, but later it was shown that a much simpler effective-medium [24, 25] description was often useful. Such a description is valid when the characteristic wavelengths of the excitation are much longer than the superlattice period. It is then possible to derive the effective-medium permeability tensor [24, 25] and dielectric tensor [26, 27]. A feature of both tensors is that they are now characteristic of anisotropic media because of the anisotropy introduced by the layered structure itself.

There have been a number of studies of magnetic polaritons in semi-infinite antiferromagnetic superlattices using effective-medium theory [28]. Some finite structures have also been examined [29]. In this paper we study the surface and guided modes that propagate in an effective-medium film on a nonmagnetic substrate. We use the Voigt configuration where the direction of propagation is perpendicular to the magnetic moments and to the applied field. We obtain analytical forms for implicit dispersion relations and show that these results reduce to previously known expressions for simpler cases. These expressions apply for both ferromagnetic and antiferromagnetic effective-medium films. A key feature of our results deals with the localization of the spin wave modes. In particular we show that guided wave modes lying within the bulk continuum of modes can still be strongly localized to one surface or another of the film. In addition we see that introducing a nonmagnetic substrate introduces a substantial nonreciprocity [30] into the dispersion relation for surface and guided wave modes, i.e.  $\omega(+\mathbf{k}) \neq \omega(-\mathbf{k})$  where  $\mathbf{k}$  is the propagation wavevector. Such a nonreciprocity does not occur for an isolated antiferromagnetic film.

The remainder of the paper is organized as follows. In section 2 we present the derivation of the general dispersion relations. In section 3 we study these relations in the nonretarded (static) limit. In section 4 we use the general dispersion relations to investigate the polaritons for effective-medium films bounded both symmetrical and asymmetrically. We give numerical examples in this section for an FeF<sub>2</sub>-ZnF<sub>2</sub> superlattice on a ZnF<sub>2</sub> substrate. In addition to the dispersion relations, we present profiles illustrating the character and localization of the surface and guided waves.

## 2. Derivation of general dispersion relations

We consider the geometry shown in figure 1. An effective-medium magnetic film is sandwiched between two dielectric media, a capping layer characterized by dielectric constant  $\epsilon_m$  and substrate having dielectric constant  $\epsilon_s$ . We restrict our attention to the Voigt geometry, with an external static magnetic field  $\mathbf{H}_0$  along the  $z$  axis. When the static magnetization lies in the  $xz$  plane, the effective-medium permeability tensor is often given by [24, 25]

$$\boldsymbol{\mu}(\omega) = \begin{pmatrix} \mu_1 & -i\mu_T & 0 \\ +i\mu_T & \mu_2 & 0 \\ 0 & 0 & \mu_3 \end{pmatrix} \quad (1)$$

where

$$\mu_1 = f_a \mu_1^a + f_b \mu_1^b - f_a f_b (\mu_2^a - \mu_2^b)^2 / (f_b \mu_1^a + f_a \mu_1^b) \quad (2a)$$

$$\mu_2 = \mu_1^a \mu_1^b / (f_b \mu_1^a + f_a \mu_1^b) \quad (2b)$$

$$\mu_3 = f_a \mu_3^a + f_b \mu_3^b \quad (2c)$$

$$\mu_T = (f_a \mu_2^\alpha \mu_1^b + f_b \mu_1^\alpha \mu_2^b) / (f_b \mu_1^\alpha + f_a \mu_1^b) \tag{2d}$$

where  $f_a$  ( $f_b$ ) is the ratio of volume occupied by the layer a (b) to the total volume of the unit cell of the specimen. Each layer  $\alpha$  ( $= a$  or  $b$ ) in the magnetic superlattice is characterized by a dielectric constant  $\epsilon_\alpha$  and a permeability tensor  $\mu^\alpha(\omega)$ , which is given by [31, 32]

$$\mu^\alpha(\omega) = \begin{pmatrix} \mu_1^\alpha & -i\mu_2^\alpha & 0 \\ +i\mu_2^\alpha & \mu_1^\alpha & 0 \\ 0 & 0 & \mu_3^\alpha \end{pmatrix}. \tag{3}$$

Here  $\mu_1^\alpha$  and  $\mu_2^\alpha$  have resonances at the corresponding ferromagnetic or antiferromagnetic resonance frequencies. Generally  $\mu_3^\alpha$  does not have a strong resonance frequency, but in canted structures such as an antiferromagnetic in a spin flop state this is not true. In the absence of damping  $\mu_1^\alpha$  is real and  $i\mu_2^\alpha$  is pure imaginary. The effective dielectric tensor  $\epsilon$  has the properties of a conventional uniaxial medium [27] with principal values  $\epsilon_\parallel$  for  $\epsilon_{xx}$  and  $\epsilon_{zz}$  and  $\epsilon_\perp = \epsilon_{yy}$ , where

$$\epsilon_\perp = f_a \epsilon_a + f_b \epsilon_b \tag{4a}$$

$$\epsilon_\parallel = \epsilon_a \epsilon_b / (f_b \epsilon_a + f_a \epsilon_b). \tag{4b}$$

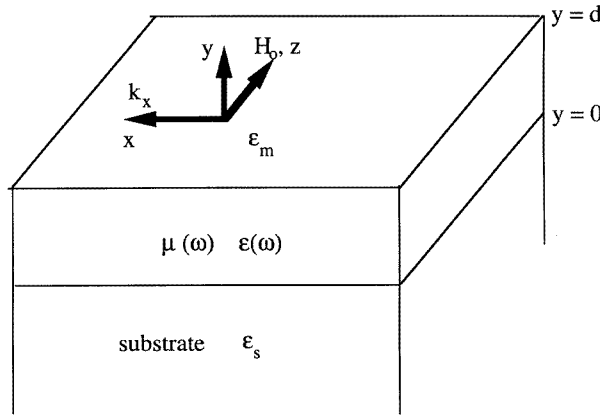


Figure 1. The geometry considered in this paper.

To find the dispersion relation, we start with Maxwell’s curl equations. After eliminating the electric field variable  $\mathbf{E}$ , we obtain the following wave equation:

$$\mathbf{k} \times \epsilon^{-1} \cdot (\mathbf{k} \times \mathbf{H}) + q_0^2 \mu(\omega) \cdot \mathbf{H} = 0 \tag{5}$$

where  $q_0 = \omega/c$  is the vacuum wavevector. In (5) we assumed a spatial and temporal dependence of the form  $\exp(i\mathbf{k} \cdot \mathbf{r} - \omega t)$ . Consequently (5) is a set of three linear homogeneous equations satisfied by the magnetic field in the effective-medium film. The same set of three equations also gives valid solutions in the isotropic medium cap and the substrate, if we just take  $\mu(\omega) \rightarrow 1$  and  $\epsilon$  goes to  $\epsilon_m$  or  $\epsilon_s$ . As is to be expected from the form of (1), the magnetic polaritons of interest are TE modes with the electric field  $\mathbf{E}$  along the  $z$  axis and the magnetic field  $\mathbf{H}$  in the  $xy$  plane. The nontrivial solution of such a set of three linear equations leads to

$$-k_y^2 = \beta^2 = (\mu_1/\mu_2)k_x^2 - q_0^2 \epsilon_\perp \mu_V \tag{6}$$

in the effective medium, and

$$-k_y^2 = \beta_i^2 = k_x^2 - q_0^2 \epsilon_i \quad i = m \text{ or } s \tag{7}$$

where  $\mu_V = (\mu_1 \mu_2 - \mu_T^2) / \mu_2$  is the Voigt permeability.

To derive the dispersion relation for the TE magnetic wave in the Voigt configuration, we seek a solution of Maxwell’s equation in the three media in the form

$$\mathbf{E} = (0, 0, E_{mz}) \exp(-\beta_m y) \quad y > +d \tag{8}$$

$$\mathbf{E} = (0, 0, E_{az}) \exp(\beta y) + (0, 0, E_{bz}) \exp(-\beta y) \quad d > y > 0 \tag{9}$$

$$\mathbf{E} = (0, 0, E_{sz}) \exp(+\beta_s y) \quad y < 0 \tag{10}$$

where  $\exp(i(k_x x - \omega t))$  is an implicit common factor in (8)–(10). Using the Maxwell equation  $\nabla \times \mathbf{E} = -(1/c) \partial \mathbf{B} / \partial t$ , the magnetic field in the three regions can be obtained. In order to have a bounded excitation, we require that  $\beta_m$  and  $\beta_s$  are both real and positive. The determination of the dispersion relation requires the match of electromagnetic boundary conditions at  $y = 0$  and  $y = d$ , namely continuity of the tangential components of the magnetic and electric field  $H_x$ ,  $H_y$ , and  $E_z$ . Using Maxwell’s equations with (5) we express the tangential components in terms of the unknowns  $E_{mz}$ ,  $E_{az}$ ,  $E_{bz}$ , and  $E_{sz}$ . The boundary conditions then yield the following dispersion relation:

$$\frac{g_+ - \beta_m(\mu_1 \mu_2 - \mu_T^2)}{g_- - \beta_m(\mu_1 \mu_2 - \mu_T^2)} \exp(-\beta d) = \frac{g_+ + \beta_s(\mu_1 \mu_2 - \mu_T^2)}{g_- + \beta_s(\mu_1 \mu_2 - \mu_T^2)} \exp(+\beta d) \tag{11a}$$

which reduces to

$$(\beta_m \beta_s (\mu_1 \mu_2 - \mu_T^2) - k_x \mu_T (\beta_s - \beta_m) + k^2) \tanh(\beta d) + \beta \mu_2 (\beta_m + \beta_s) = 0 \tag{11b}$$

where  $g_{\pm} = \mu_T k_x \pm \mu_2 \beta$  and  $k^2 = k_x^2 - q_0^2 \epsilon_{\perp} \mu_2$ . Equations (11) above constitute the main analytical results of the work. We have checked (11) by imposing various special limits, viz.,  $d = 0$  and  $d \rightarrow \infty$ . It is found that within these special limits the general dispersion relation (11) reproduces exactly the results previously reported, for a single interface ( $d = 0$ ; see e.g. [33]) and ( $d \rightarrow \infty$  [24, 25]).

Depending on the spectral region  $\beta$ ,  $\beta_m$ , and  $\beta_s$  can be real or imaginary. In order to have bounded excitations we must have  $\beta_m$  and  $\beta_s$  both be real and positive. This corresponds to electric fields that vanish exponentially as one moves away from the film. If, in addition,  $\beta$  is real then we have a surface mode that decays exponentially both inside and outside the effective-medium film. If  $\beta$  is imaginary, then we have bulk modes, with an oscillatory profile for the electric field inside the film. As we will see, this division into bulk and surface modes is somewhat arbitrary. There are cases where an individual mode technically changes form a surface mode to a bulk mode, but still retains most of its properties, particularly with regard to being localized to a particular surface.

The case of TM polarization, with  $\mathbf{H}$  along the  $z$  axis, may also be of interest for canted structures as discussed previously. The dispersion relations for this case may be obtained in a similar fashion. We find

$$(\beta_m \beta_s \epsilon_{\perp} + \beta^2) \tanh(\beta d) + \epsilon_{\perp} \beta (\beta_m + \beta_s) = 0 \tag{12}$$

where now

$$-k_y^2 = \beta^2 = (\epsilon_{\perp} / \epsilon_{\parallel}) k_x^2 - q_0^2 \epsilon_{\perp} \mu_3. \tag{13}$$

### 3. The magnetostatic limit

In the magnetostatic limit  $k_x \gg q_0$ , the decay constants reduce to  $\beta_m = \beta_s = k = |k_x|$  and

$$\beta = (\mu_1/\mu_2)^{1/2}k_x. \quad (14)$$

Equation (11) then reduces to

$$(\mu_1\mu_2 - \mu_T^2 + 1) \tanh((\mu_1/\mu_2)^{1/2}|k_x|d) + 2\mu_2(\mu_1/\mu_2)^{1/2} = 0. \quad (15)$$

(15) indicates that the dispersion relation in the magnetostatic limit is reciprocal, independent of the dielectric substrate. In the limit of  $f_a = 1$ , (15) reduces to equation (23) in [10] and equation (25) in [11].

One can analyse (15) in the following special cases:

(i)  $k_x d \gg 1$ . The hyperbolic tangent in (15) tends to unity, hence (15) reduces to two conditions,

$$(\mu_1\mu_2)^{1/2} + \mu_T + 1 = 0 \quad (16)$$

$$(\mu_1\mu_2)^{1/2} - \mu_T + 1 = 0. \quad (17)$$

Equations (16) and (17) for  $f_a = 1$  together with  $d \rightarrow \infty$  reproduce exactly the result previously obtained for the semi-infinite system [34].

(ii)  $k_x d \ll 1$ . Assuming that  $(\mu_1/\mu_2)^{1/2}k_x d \ll 1$  then (15) yields an explicit solution for  $k_x$ ,

$$|k_x| = -2\mu_2/d(\mu_1\mu_2 - \mu_T^2 + 1). \quad (18)$$

This result holds for very thin films.

### 4. The retarded limit

#### 4.1. A symmetrically bounded effective-medium film

For the symmetric configuration, when  $\varepsilon_m$  and  $\varepsilon_s$  are both equal to, say,  $\varepsilon$ , and therefore  $\beta_m = \beta_s$ , then (11) reduces to the following dispersion relation:

$$(\beta_s^2\mu_V^2 + \beta^2 - (\mu_T/\mu_2)^2k_x^2) \tanh(\beta d) = -2\beta_s\beta\mu_V. \quad (19)$$

As  $d \rightarrow \infty$ , the hyperbolic function in (19) tends to unity and (19) yields two conditions, the dispersion relation for the single interface effective mode [24, 25]:

$$\beta_s\mu_V + \beta \pm (\mu_T/\mu_2)k_x = 0. \quad (20)$$

We note that even though the dispersion relation is reciprocal, the mode profile of the wave may be nonreciprocal, i.e. the localization of the wave to the upper or lower surface depends on propagation direction. We will see explicit example of this below. Also (19) for  $f_a = 1$  reduces to equation (12) in [12].

We have solved the implicit dispersion relation given by (19) numerically. We use the parameters and the permeabilities defined in [28] for the antiferromagnetic FeF<sub>2</sub>. This gives a resonance frequency  $\omega_0 = \gamma(2H_a H_e + H_a^2)^{1/2} = 260$  GHz. The results, frequency as a function of wavevector for different values of the filling fraction  $f_a$ , are presented in figure 2. The thickness of the film is 200  $\mu\text{m}$ .

In figure 2(a) we show the results for  $f_a = 1$ , i.e. a pure FeF<sub>2</sub> film. For orientation, the limits of the bulk band in an infinite extended antiferromagnet are also shown as dotted lines. Because of the finite film thickness, the bulk modes are quantized, corresponding to different standing waves within the film. As a result the bulk ‘band’ is now broken

up into individual modes, as expected, and as previously described by Lacy. The surface modes in the middle of the figure exist outside the bulk bands. In contrast, the surface modes at the top of the figure ( $\omega/\omega_0 = 1.01$ ) continue smoothly from outside the bulk band limits to inside these limits. As we will see, in the regions where the surface mode penetrates into the bulk band, we obtain mixed type modes having both bulk and surface characteristics.

In figure 2(b)–(d) we show the evolution of the dispersion curves as  $f_a$  is decreased, i.e. as more nonmagnetic material is introduced. In the study of surface modes on antiferromagnetic superlattices, it was argued that as  $f_a > 0.5$  the magnetostatic modes (the surface modes which exist for  $k \rightarrow \infty$ ) disappear because the surface modes intersect the bulk band. In our results for thin films, we see that the surface modes penetrate the bulk bands, but, in fact, remain relatively far away from the quantized bulk modes over much of the  $k$ -space. Thus even for figure 2(d) where the ‘surface modes’ are mostly contained in the bulk band, they really maintain their identity as individual modes.

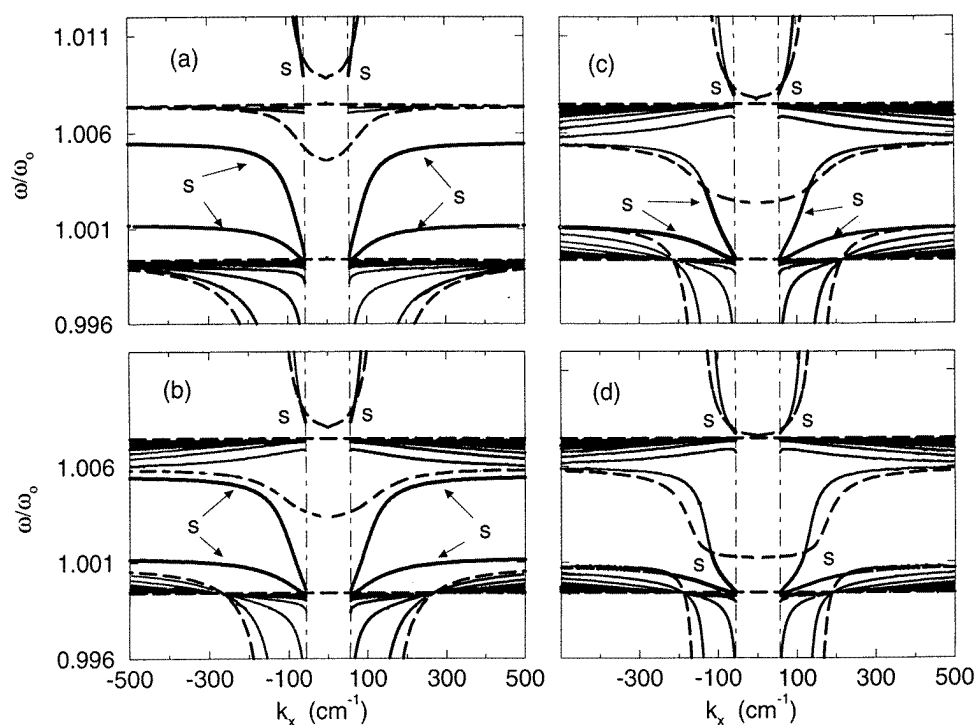


**Figure 2.** Dispersion relations for magnetic polaritons of an effective-medium film in vacuum. The heavy dashed lines show the boundaries of the bulk bands in an infinite effective medium. The nearly vertical dashed lines are the light lines in vacuum. (a)  $f_a = 1$ , corresponding to a pure  $\text{FeF}_2$  film; (b)  $f_a = 0.7$ ; (c)  $f_a = 0.5$ ; (d)  $f_a = 0.3$ . The applied field is 0.2 kG and the thickness of the film is  $200 \mu\text{m}$ .

In figure 3 we illustrate the character of the modes by plotting  $|E_z(y)|^2$  within the antiferromagnetic film. These plots are for  $f_a = 0.5$ . In figure 3(a) we study the high-frequency surface mode, just outside the upper bulk band. The  $+k_x$  and  $-k_x$  modes are essentially mirror images of each other, with the localization exactly reversed by a reversal

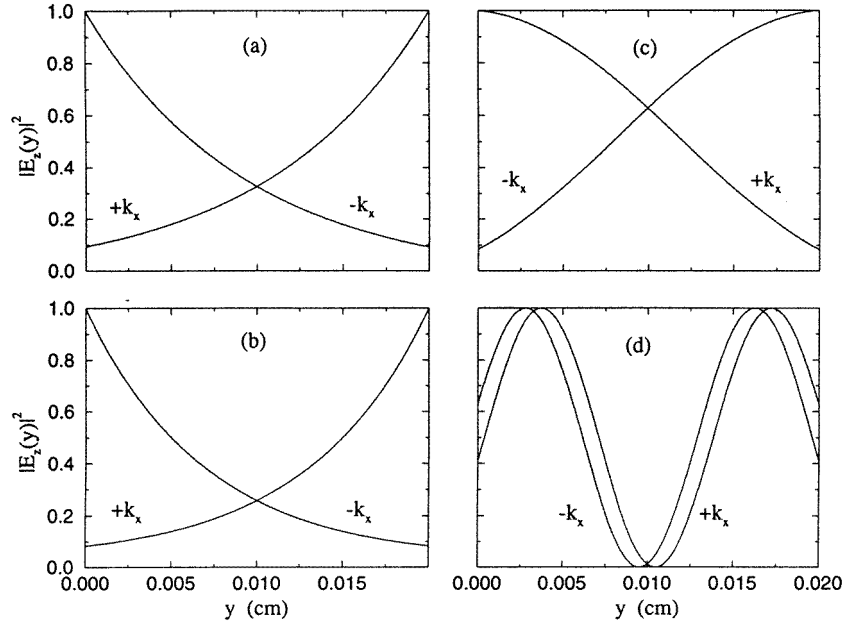


**Figure 3.** Electric field profiles for different points on the dispersion relation of figure 2(c): (a)  $k_x = 61 \text{ cm}^{-1}$  and  $\omega/\omega_0 = 1.008216$ ; (b)  $k_x = 113 \text{ cm}^{-1}$  and  $\omega/\omega_0 = 1.002045$ ; (c)  $k_x = 200 \text{ cm}^{-1}$  and  $\omega/\omega_0 = 1.004817$ ; (d)  $k_x = 89 \text{ cm}^{-1}$  and  $\omega/\omega_0 = 0.9980063$ .  $y = 0$  corresponds to the antiferromagnet–substrate interface.

of the direction of propagation. This is true of all the modes in this symmetric structure. This is to be expected since a reversal of propagation is essentially equivalent to rotating the film through  $180^\circ$  about the external magnetic field.

We examine the surface mode in the middle of the dispersion curve ( $\omega/\omega_0 = 1.004$ ) in figure 2(b) and (c). In (b) the surface mode lies outside the bulk band and the profile is characteristic of exponential functions, i.e.  $\beta$  is pure real. In (c) we are looking at the profile for the same surface mode that has now penetrated the bulk band. As a result  $\beta$  is imaginary and the profiles show features characteristic of sines and cosines. However, the wave remains strongly localized to one surface or the other. The three curves for surface modes, figure 3(a)–(c), all display significant localization, while the one curve, figure 3(d), for a bulk mode displays a profile which has intensity at the two surfaces which is nearly the same.

In the dispersion relation of figure 2, the results are reciprocal in the sense that  $\omega(k_x) = \omega(-k_x)$ ; the frequency is independent of the direction of propagation. However, the localization of the wave depends strongly on the sign of  $k_x$  as can be seen in figure 3. In all cases, reversing the direction of propagation reverses the localization of the wave as well.

#### 4.2. An asymmetrically bounded effective medium film

The case investigated here, an antiferromagnetic film on a substrate, is obviously more practical. In figure 4 we present the dispersion relations, again for different values of  $f_a$ . The introduction of the substrate has immediate consequences for the dispersion relations.



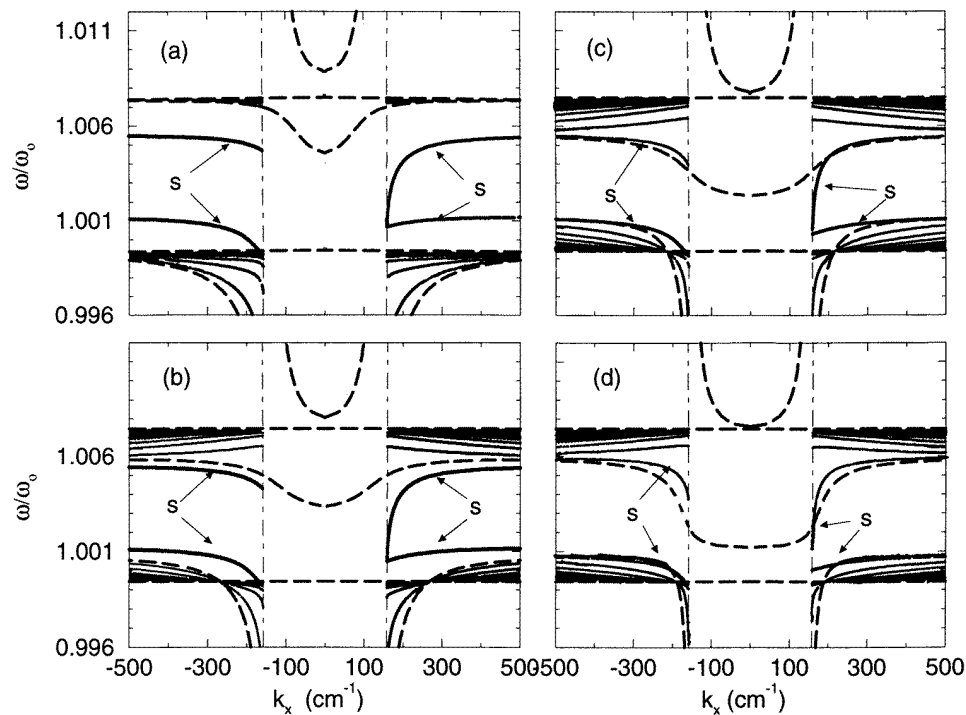


**Figure 4.** Dispersion relations for magnetic polaritons of an effective-medium film on a substrate: (a)  $f_a = 1$ , corresponding to a pure  $\text{FeF}_2$  film; (b)  $f_a = 0.7$ ; (c)  $f_a = 0.5$ ; (d)  $f_a = 0.3$ . The applied field is 0.2 kG and the thickness of the film is 200  $\mu\text{m}$ . The nearly vertical dashed lines are the light lines for the substrate.

Since the substrate has a high dielectric constant, the light line  $\omega = ck/\varepsilon^{1/2}$ , that marks the boundary of the bounded modes, now lies farther out in  $k_x$ -space. More importantly, the dispersion curves, particularly for the surface modes, are now strongly nonreciprocal. This nonreciprocity persists even as the fraction of the magnetic material  $f_a$  is reduced.

It is easy to understand why the introduction of a substrate should create such nonreciprocity in the surface modes. In the previous section we saw that, depending on the sign of  $k_x$ , these waves were localized either to the top surface of the film or the bottom surface of the film. When the wave is localized to the top surface, it has the dispersion relation of a surface mode appropriate to a vacuum–antiferromagnetic interface. When the wave is localized to the bottom surface, it has the dispersion relation appropriate to the dielectric–antiferromagnetic interface.

The strongest nonreciprocity in the asymmetric structure occurs near the light line. Again this is easy to understand. At large wavevectors, far away from the light line, the excitations are essentially decoupled from the electromagnetic waves and are representative of the pure magnetic spin waves. In this case, the dielectric constant of the substrate becomes unimportant, because the waves have essentially no electric field component to be influenced by the dielectric constant.

In figure 5 we plot the profiles of some of the waves in figure 4(c). Note that since the dispersion relations are no longer reciprocal, we must choose different frequencies for  $+k_x$  and  $-k_x$  propagation in order to remain on the dispersion curves. A very interesting

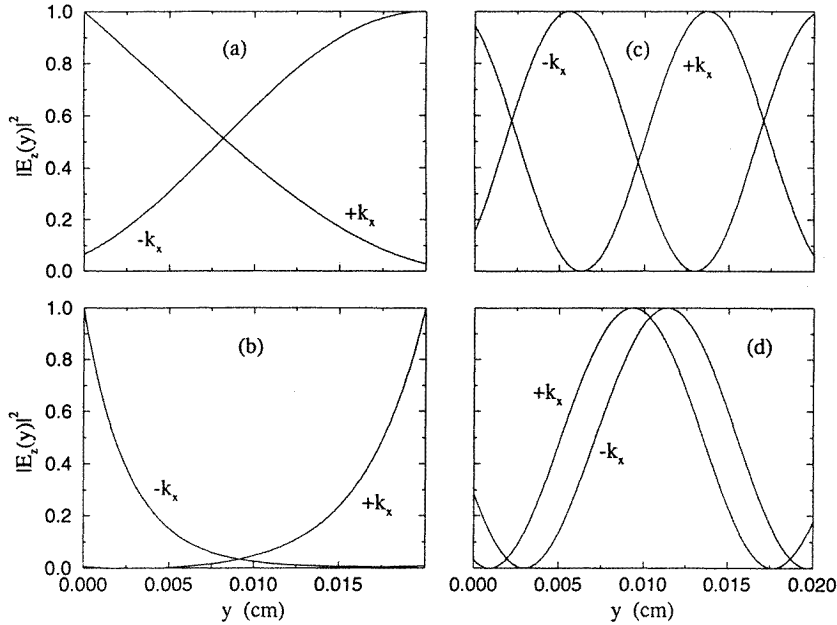


**Figure 5.** Electric field profiles for different points on the dispersion relation of figure 4(c): (a)  $k_x = +250 \text{ cm}^{-1}$  and  $\omega/\omega_0 = 1.004963$  and  $k_x = -250 \text{ cm}^{-1}$  and  $\omega/\omega_0 = 1.00512$ ; (b)  $k_x = 190 \text{ cm}^{-1}$  and  $\omega/\omega_0 = 1.000507$  and  $k_x = -190 \text{ cm}^{-1}$  and  $\omega/\omega_0 = 0.9998679$ ; (c)  $k_x = \pm 351 \text{ cm}^{-1}$  and  $\omega/\omega_0 = 1.006006$ ; (d)  $k_x = \pm 351 \text{ cm}^{-1}$  and  $\omega/\omega_0 = 1.000374$ .  $y = 0$  corresponds to the antiferromagnet–substrate interface.

consequence of this is shown in figure 5(a). Here we present profiles of the modes for  $k_x = \pm 250$  and frequencies near  $\omega/\omega_0 = 1.005$ . On one side of figure 4(c) ( $+k_x$ ), the mode is a true surface mode. The resultant profile in figure 5(a) has exponential characteristics. On the other side of the dispersion relation ( $-k_x$ ) the mode lies inside the bulk band. As a result the profile of this mode in figure 5(a) appears more like a portion of a bulk mode. Nonetheless, both the ‘true’ surface mode and the ‘bulk’ mode show strong localization to one surface or the other, with the  $-k_x$  mode being localized at the vacuum–antiferromagnet interface and the  $+k_x$  mode being localized at the antiferromagnet–substrate interface.

An interesting feature of the profiles is that the bulk ‘standing waves’ also can show significant localization. For example in figure 5(c) the  $+k_x$  mode has a large intensity on the  $y = 0$  side of the film (the substrate side) and a much smaller intensity on the  $y = 0.02 \text{ cm}$  side. The mode for  $-k_x$  has this localization reversed. A much weaker localization is evident in the bulk mode shown in figure 5(d).

## 5. Summary and conclusions

We have obtained the general dispersion relation for magnetic polaritons propagating in an effective-medium film supported by a nonmagnetic substrate. The general results are applied in a study of polaritons in an antiferromagnet–nonmagnet superlattice of  $\text{FeF}_2$ – $\text{ZnF}_2$  on a  $\text{ZnF}_2$  substrate. Two key results emerge. (i) In the presence of a substrate the dispersion relations for the surface modes of the effective-medium film are markedly nonreciprocal. This is in contrast to the results for a free-standing film. (ii) The field profiles

of the polaritons show that even when surface modes penetrate the bulk band region, they maintain a high degree of localization. Reversing the direction of propagation changes the localization from one surface to the other.

### Acknowledgments

The work of REC was supported by US ARO grant No DAAH04-94-G-0253 and by EPSRC. The authors would also like to thank D R Tilley and R Loudon for helpful discussions.

### References

- [1] Walker L R 1957 *Phys. Rev.* **105** 390
- [2] Wallis R F, Brion J J, Burstein E and Hartstein A 1974 *Phys. Rev. B* **9** 3424
- [3] Ushioda S and Loudon R 1982 *Surface Polaritons* ed V M Agranovich and D L Mills (Amsterdam: North-Holland)
- [4] Kuswaha M S and Halevi P 1987 *Phys. Rev. B* **35** 3879
- [5] Kuswaha M S and Halevi P 1987 *Phys. Rev. B* **36** 5960
- [6] Kuswaha M S and Halevi P 1987 *Phys. Rev. B* **38** 12428
- [7] Kuswaha M S and Halevi P 1987 *Solid State Commun.* **64** 1405
- [8] Elmszugi F G and Tilley D R 1994 *J. Phys.: Condens. Matter* **6** 4233
- [9] Elmszugi F G 1995 *J. Phys.: Condens. Matter* **7** 7023
- [10] Damon R W and Eshbach J R 1961 *J. Phys. Chem. Solids* **19** 308
- [11] Karsono A D and Tilley D R 1978 *J. Phys. C: Solid State Phys.* **11** 3487
- [12] Marchand M and Caille A 1980 *Solid State Commun.* **34** 827
- [13] Camley R E and Mills D L 1982 *Phys. Rev. B* **26** 1280
- [14] Shu C and Caillé A 1982 *Solid State Commun.* **42** 233
- [15] Stamps R L and Camley R E 1989 *Phys. Rev. B* **40** 596
- [15] Stamps R L and Camley R E 1989 *Phys. Rev. B* **40** 609
- [16] Remer L, Lüthi B, Sauer H, Geick R and Camley R E 1986 *Phys. Rev. Lett.* **56** 2752
- [17] Brown D E, Dumelow T, Parker T J, Abraha K and Tilley D R 1994 *Phys. Rev. B* **49** 12266
- [18] Abraha K, Brown D E, Dumelow T, Parker T J and Tilley D R 1994 *Phys. Rev. B* **50** 6808
- [19] Jensen M R F, Parker T J, Abraha K and Tilley D R 1995 *Phys. Rev. Lett.* **75** 3756
- [20] Ramos C A, Lederman D, King A R and Jaccarino V 1990 *Phys. Rev. Lett.* **65** 2913
- [21] Borchers J A, Carey M J, Erwin R W, Majkrzak C F and Berkowitz A E 1993 *Phys. Rev. Lett.* **70** 1878
- [22] Abarra A 1996 private communication
- [23] Camley R E, Rahman T S and Mills D L 1983 *Phys. Rev. B* **27** 261
- [24] Raj N and Tilley D R 1987 *Phys. Rev. B* **36** 7003
- [25] Almeida N S and Mills D L 1988 *Phys. Rev. B* **38** 6698
- [26] Agranovich V M and Kravtsov V E 1985 *Solid State Commun.* **55** 373
- [27] Raj N and Tilley D R 1985 *Solid State Commun.* **55** 533
- [28] Oliveros M C, Almeida N S, Tilley D R, Thomas J and Camley R E 1992 *J. Phys.: Condens. Matter* **4** 8497 and references therein
- [29] Lacy F, Carter E L and Richardson S L 1993 *Mater. Res. Soc. Symp. Proc.* vol 313 (Pittsburgh, PA: Materials Research Society) p 65
- [30] Camley R E 1987 *Surf. Sci. Rep.* **7** 103
- [31] Mills D L 1984 *Surface Excitations* ed V M Agranovich and R Loudon (Amsterdam: North-Holland) p 379
- [32] Camley R E and Cottam M G 1987 *Phys. Rev. B* **35** 189
- [33] Cottam M G and Tilley D R 1989 *Introduction to Surface and Superlattice Excitations* (Cambridge: Cambridge University Press)
- [34] Hartstein A, Burstein E, Maradudin A A, Brewer R and Wallis R F 1973 *J. Phys. C: Solid State Phys.* **6** 1266